

Correlation of Himalayan exhumation rates and Asian monsoon intensity

PETER D. CLIFT^{1*}, KIP V. HODGES², DAVID HESLOP³, ROBYN HANNIGAN⁴, HOANG VAN LONG¹
AND GEROME CALVES¹

¹Department of Geology and Petroleum Geology, University of Aberdeen, Aberdeen AB24 3UE, UK

²School of Earth and Space Exploration, Arizona State University, PO Box 871404, Tempe, Arizona 85287-1404, USA

³F.B. Geowissenschaften, Universität Bremen, Klagenfurter Strasse, 28359 Bremen, Germany

⁴Department of Chemistry and Physics, Arkansas State University, State University, Arkansas 72467, USA

*e-mail: p.clift@abdn.ac.uk

Published online: 9 November 2008; doi:10.1038/ngeo351

Although most data suggest that the India–Eurasia continental collision began ~45–55 Myr ago, the architecture of the Himalayan–Tibetan orogen is dominated by deformational structures developed in the Neogene period (<23 Myr ago). The stratigraphic record and thermochronometric data indicate that erosion of the Himalaya intensified as this constructional phase began and reached a peak around 15 Myr ago. It remained high until ~10.5 Myr ago and subsequently slowed gradually to ~3.5 Myr ago, but then began to increase once again in the Late Pliocene and Pleistocene epochs. Here we present weathering records from the South China Sea, Bay of Bengal and Arabian Sea that permit Asian monsoon climate to be reconstructed back to the earliest Neogene. These indicate a correlation between the rate of Himalayan exhumation—as inferred from published thermochronometric data—and monsoon intensity over the past 23 Myr. We interpret this correlation as indicating dynamic coupling between Neogene climate and both erosion and deformation in the Himalaya.

There is general consensus that the India–Eurasia continental collision began around 45–55 Myr ago with closure of the Neotethys Ocean¹. The great thickness of crust beneath Tibet and the Himalaya testify to progressive convergence between India and Eurasia since that time, but geologists have limited information regarding the early stages of the collisional process. Sedimentary deposits shed from the rising Himalaya date back to the Middle–Late Eocene epoch (49–34 Myr ago), providing indirect evidence for early mountain building^{2,3}. Thermobarometric and geochronologic data demonstrate that this deformation was accompanied by metamorphism associated with crustal thickening^{4,5}, and a few pre-Neogene structures have been identified on the northern flank of the Himalaya in the southernmost Tibetan plateau^{6,7}. However, throughout the Greater Himalaya, the most significant deformation and the most intensive metamorphic and magmatic activity took place since 23 Myr ago. The stratigraphic record in the Himalayan foreland basin, located south of the ranges, as well as in the main sediment repositories of the Indus and Bengal fans, also indicates that the greatest erosional fluxes from the developing Himalaya occurred during the Neogene^{8–10}.

An important unresolved question, then, is why exhumation of high-grade metamorphic rocks, such as seen in the Greater Himalaya, did not take place until 15–20 Myr after the India–Eurasia collision began. Here, we present new climate records that show that the rise of the Himalaya was related temporally—and perhaps genetically—to the intensification of Asian monsoons.

RECONSTRUCTING THE ASIAN MONSOONS

The age of inception of the East and South Asian monsoons remains controversial, but a variety of environmental indicators suggest that the East Asian monsoon, at least, was established by the beginning of the Neogene (~24 Myr ago). For example, a major reorganization of environmental belts in China around ~24 Myr ago probably indicates establishment of a monsoon climate¹¹. Furthermore, alternating layers of eolian dust and soils formed by periods of stronger and weaker summer monsoon started to collect in the Chinese loess plateau no later than 22 Myr ago¹², and possibly as early as 29 Myr (ref. 13), implying that climate patterns in the region resembled their modern form before 22 Myr ago. Fortunately, the marginal basins of Asia contain a rich Neogene stratigraphic record. We can capitalize on that record to monitor the evolution of the monsoons by looking at indications of increases in chemical and physical weathering rates which, depending on the physiography of the source regions of the sediment, indicate wetter or drier climates.

On the continents, precipitation, temperature and vegetation are the primary controls on both chemical weathering and physical erosion^{14–16}. On geologic timescales, a measure of this is preserved in the chemistry and mineralogy of sediments transported by rivers. Chemical and mineralogical indices that have been used to monitor the intensity of chemical weathering include the Chemical Index of Alteration¹⁷ (CIA), the mineralogical ratio chlorite/(chlorite + haematite + goethite) (C_{RAT}) and the K/Al ratio (see Supplementary Information, Discussion). Different

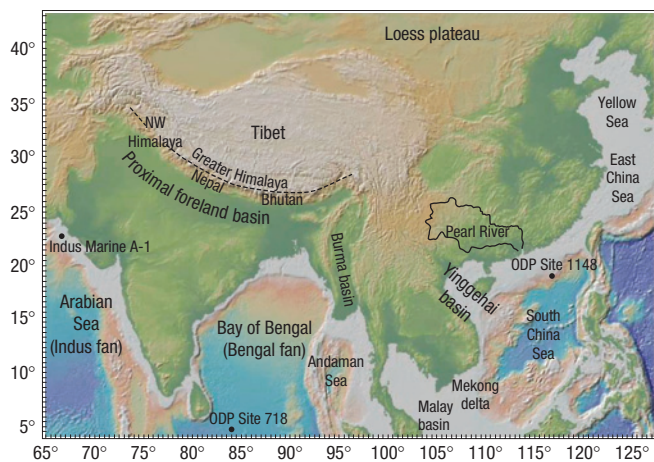


Figure 1 Physiographic map of Asia with study sites. The map shows the locations of ODP Site 718 and Site 1148, well Indus Marine A-1, the marginal basins used for the sediment flux graph in Fig. 2d, the Himalayan hinterland and the location of the Nepal foreland basin. The arc of the Greater Himalayan range is shown by the dashed line.

indices are more valuable (and more reliable) in some settings than in others.

The chemistry of sediments in eastern Himalayan rivers indicates that runoff, rather than temperature, is the dominant weathering control in the modern system¹⁸. Most precipitation in the continental interiors of India and China is introduced by seasonal storms of the South and East Asian monsoons, which thus control runoff. In areas of limited topographic relief, strong monsoon precipitation is likely to be the principal driver of enhanced chemical weathering¹⁸. In these areas, a higher degree of chemical weathering indicates a wetter climate and thus a stronger monsoon. Unfortunately, most major river systems in South and East Asia drain regions of high relief, where greater runoff not only increases chemical weathering but also physical erosion¹⁹, which dilutes the products of chemical weathering. To use stratigraphy to track the intensity of the Asian monsoons, we begin by exploring the record from a part of Asia that has been strongly affected by monsoon climate since the start of Himalayan–Tibetan orogenesis, but that does not include mountainous regions that developed over that time frame.

Sedimentary basins in the South China Sea preserve some of the best stratigraphic records available for the continental interior of eastern Asia. A core from Ocean Drilling Program (ODP) Site 1148 in the South China Sea represents a nearly complete sequence of essentially unaltered²⁰ Neogene sediments eroded from the Pearl River system in southern China (Fig. 1) (see Supplementary Information, Fig. S1). In contrast with other major river systems in this part of the world that have their sources in the Tibetan plateau, the Pearl River today exclusively drains low-relief regions. Nd isotopic data for the sediments in the Site 1148 core indicate that this was also the case throughout the Neogene²¹. As a consequence, we regard the weathering history recorded at Site 1148 as indicative of variations in regional climate—specifically the East Asian monsoon climate—and not tectonic activity.

Figure 2a illustrates C_{RAT} variations in the Site 1148 core; higher values imply a wetter climate. The overall trend is one of gradually increasing monsoon strength from the beginning of the Neogene to 10.0 Myr ago, with an unusually dry period between 16.5 and 15.0 Myr. From 10.0 to 3.5 Myr ago, monsoon intensity

decreased, only to increase thereafter. Notably, the indication of Late Pliocene–Holocene monsoon intensification in these data is corroborated by other climate proxies²². Nonetheless, weathering is never again as strong as it was in the Middle Miocene period, possibly because of the extra influence of higher temperatures during the climatic optimum²³. This same pattern is corroborated by variations in K/Al (see Supplementary Information, Discussion and Supplementary Information, Fig. S4). However, the CIA index suggests a long, steady decline in East Asian monsoon intensity throughout the Neogene, at odds with virtually all independent evidence²⁴. The most likely explanation for this is that the bulk chemistry is not controlled by clay mineralogy but is particularly affected by the strong carbonate provenance of the Pearl River.

Assuming that the C_{RAT} and K/Al are reliable proxies, do the Site 1148 results reflect the Asian monsoon climate in general, or simply the climatic history of southern China? To answer this question, we turn to other offshore deposits eroded from regions in which the South Asian monsoon dominates the climate. Petroleum well Indus Marine A-1, for example, was drilled offshore the Indus delta (Fig. 1). The sediments in this well represent the erosion of the western Himalayas over the period 17.0–3.0 Myr ago. In these source regions, we expect a stronger monsoon to cause more intense physical erosion. Both the K/Al and CIA indices suggest a strong monsoon over the 16.0–10.0 Myr interval, followed by a gradual weakening between 10.0 and 3.0 Myr (Fig. 2b). This pattern is consistent with the Site 1148 C_{RAT} and K/Al indicators.

Further constraints on the South Asian monsoon can be derived from ODP Site 718 in the southern Bay of Bengal (Fig. 1). Sediments here were delivered through the Ganges–Brahmaputra delta and thus reflect Himalayan physical erosion throughout the 17 Myr record in the core²⁵. Despite an incomplete signal with considerable high-frequency noise caused by turbidite sands, the K/Al record for the Site 718 core, like the Indus and South China records, implies a brief dry period around 16.5 and 15.0 Myr ago, followed by high precipitation until about 10 Myr ago and then a gradual decrease in monsoon strength to 3 Myr ago. This weathering record is consistent with Sr isotope and clay mineral data from the same core, suggesting a weaker summer monsoon after 8 Myr ago²⁶. The CIA index is broadly consistent with this scenario, but is noisy, at least in part because of the low resolution and mixture of lithologies considered in that study²⁷.

We conclude that, on million-year timescales, monsoon strength varies largely in parallel in East and South Asia, with strong summer monsoons in the Middle Miocene, albeit with weakening starting earlier, around 10 Myr ago, in East Asia compared with weakening at 8 Myr ago in South Asia. This apparent time lag may reflect the importance of processes other than Himalayan orogenesis and Tibetan plateau uplift in South Asian monsoon evolution. For example, numerical models suggest that African orography may have had some impact on South Asian monsoon intensity²⁸, but minimal effect on the East Asian monsoon. Because weathering records in South Asia do not extend beyond 17 Myr ago, we are unfortunately not able to compare East Asian and South Asian monsoon proxies in more detail. However, the available data argue in favour of coupling of the systems for the past 17 Myr at least, so we suggest that it is reasonable to infer that the two were also coupled earlier.

Most sediment deposited offshore Asia was eroded from the highlands of the Himalayan–Tibetan orogen, not tectonically quiescent regions such as the Pearl River basin. In mountainous regions, the combination of high topographic relief and intense precipitation drives aggressive erosion, so we would expect a correlation between sediment flux to the oceans surrounding Asia (Fig. 1) and monsoon intensity. Although a post-4 Myr peak in sediment flux has been recognized for some time²⁹, recent

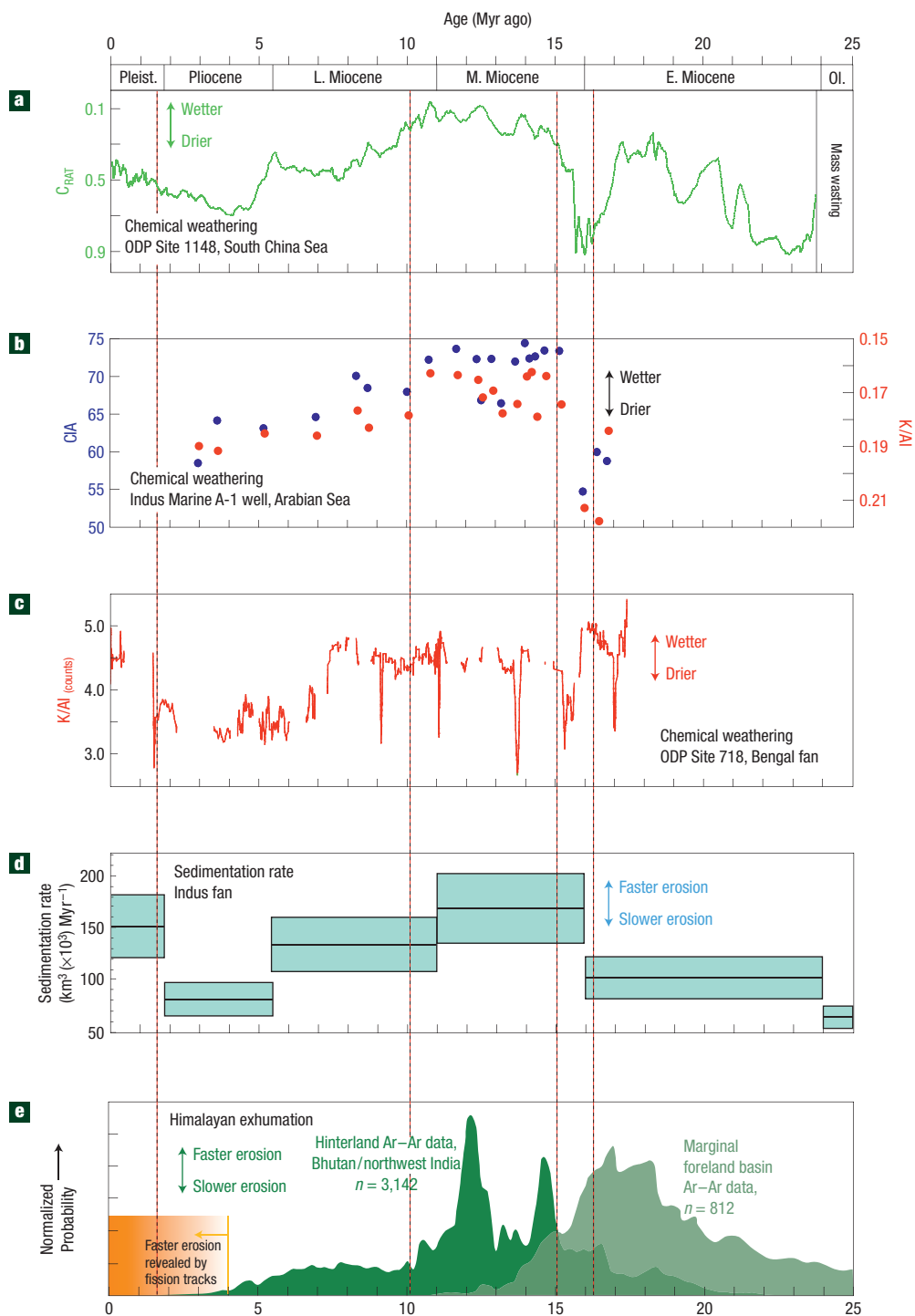


Figure 2 Correlation of erosional and depositional histories with the ODP Site 1148 monsoon intensity model. **a**, The chemical weathering index C_{RAT} (errors ± 0.1) as a function of time. **b**, K/Al ratios and CIA data from cuttings from well Indus Marine A-1. **c**, K/Al ratios from whole-core XRF scanning from ODP Site 718. **d**, Total sediment flux into the Indus fan⁹. Blue bands indicate uncertainties associated with sediment compaction calculations. **e**, Probability densities for $^{40}\text{Ar}/^{39}\text{Ar}$ muscovite dates from the Himalayan hinterland and proximal foreland. Vertical dashed lines across all frames indicate boundaries between periods of dominantly weak or strong summer monsoon. The geologic timescale is calibrated as recommended by Gradstein *et al.*⁴⁸ using the age model of the Shipboard Scientific Party⁴⁹ for Site 1148 and Gartner⁵⁰ for Site 718.

evidence also suggests an increased flux in the Early and Middle Miocene⁹ (Fig. 2e), followed by a decrease in the Late Miocene. The Middle Miocene high flux in the Indus fan was coeval with high sedimentation rates in the proximal foreland basins

of the Himalaya⁸. Unfortunately, sedimentation rates from the Bengal fan are only constrained by data from ODP Site 717 and Site 718 (ref. 30), which may not be representative of the total flux. Nonetheless, they at least corroborate the Indus record in

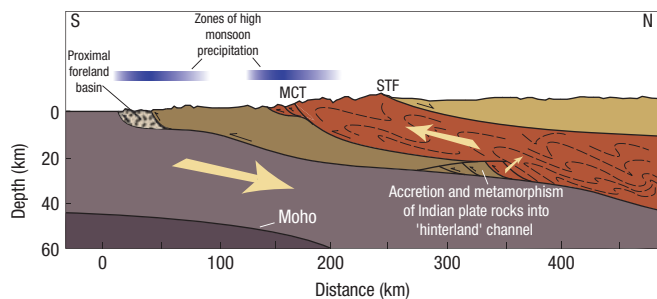


Figure 3 Schematic cross-section of the southern margin of the Himalayan–Tibetan orogen. The diagram illustrates the proposed southward channel flow of the Himalayan metamorphic hinterland from beneath the southern Tibetan plateau (at the northern side of the section). Note the vertical exaggeration indicated by horizontal and vertical scales. Important structural features mentioned in the text are the South Tibetan fault (STF) and Main Central Thrust (MCT) systems. Large arrows indicate relative transport directions of the downgoing Indian plate and the hinterland channel (shown in brick red).

showing a decrease in sediment flux after 8 Myr ago³¹. Farther afield, sedimentation records for East Asian basins have been shown to parallel the Indus fan record in showing fluxes that peak in the Middle Miocene and decrease during the Late Miocene⁹. Overall, the available sedimentation records are what would be predicted by monsoon intensity models derived from the borehole chemistry data shown in Fig. 2a–d.

RECONSTRUCTING HIMALAYAN EXHUMATION

Thermochronometric studies of detrital minerals provide valuable records of the erosional history of mountain belts. The most comprehensive data set of this kind from the Himalaya comprises muscovite $^{40}\text{Ar}/^{39}\text{Ar}$ (MAr) dates, which are generally interpreted as recording the last time at which a dated muscovite cooled through a temperature of $\sim 350^\circ\text{C}$ (ref. 32). On regional scales, such cooling typically occurs as a consequence of erosional exhumation, so that the results of thermochronometric studies are usually interpreted as indicative of the timing of active erosion. The probability density curves in Fig. 2e represent nearly 4,000 individual $^{40}\text{Ar}/^{39}\text{Ar}$ dates obtained by a variety of research groups (see Supplementary Information, Methods). The foreland curve shows one of the most recent detrital muscovite data sets ($n = 812$) from foreland basin sediments from southwest Nepal³³ (Fig. 1), which range in depositional age from 16 to 1 Myr ago. The ‘hinterland’ curve illustrates both the cooling ages of muscovites sampled from bedrock exposures in the high Himalaya, as well as detrital muscovites from modern rivers that drain these mountains in Bhutan, Nepal and northwest India (Fig. 1). Higher values on these curves indicate a higher frequency of dates in the respective data sets, and thus the timing of more aggressive bedrock erosion.

The foreland sedimentary record suggests a gradual increase in Himalayan erosion from 24 to 18 Myr, at a time of strengthening monsoons. Thereafter, the erosion rate as recorded in the foreland record seems to decrease³³. Relatively few muscovite dates from the foreland deposits are younger than 17 Myr ago. This is not the case for muscovites sampled from mountain bedrock exposures and active fluvial systems that drain these exposures; MAr dates for such samples show maximum frequency between ~ 14 and ~ 10 Myr ago. Most significantly, the Early Miocene increase in erosion rate, and subsequent 17–15 Myr decrease, track closely with monsoon intensity. Foreland data indicate a major period

of exhumation in the Early Miocene, temporally coincident with early intensification of chemical weathering, whereas the hinterland data indicate a major period of exhumation that coincided with: (1) high-intensity chemical weathering recorded at Site 718 and Site 1148 and Indus Marine A-1 and (2) high sediment flux to the Asian marginal seas. We interpret this correlation as indicative of a possible genetic relationship between monsoon intensification and Himalayan exhumation.

The lack of evidence for rapid, Late Pliocene–Pleistocene exhumation in the MAr data, despite chemostratigraphic evidence for higher monsoon activity at that time, is noteworthy. The simplest explanation is that the amount of exhumation over the past ~ 3.5 Myr has not yet been sufficient to be expressed in the MAr data. Other, lower-temperature thermochronometers are more responsive to very recent exhumation. For example, fission-track dates for the minerals zircon (ZFT) and apatite (AFT) estimate the time of cooling through nominal temperatures of $\sim 230^\circ\text{C}$ and $\sim 120^\circ\text{C}$, respectively³⁴. Far fewer ZFT and AFT dates than MAr dates have been published for the Himalaya, but the data that are available (see Supplementary Information, Methods) show that 76% of compiled bedrock ZFT and AFT dates are younger than 3.5 Myr ago (Fig. 2e), consistent with accelerated, monsoon-driven erosion since Late Pliocene time³⁵.

If Himalayan exhumation correlates closely with monsoon intensity, the climate proxies in Fig. 2a–d would predict that hinterland erosion rates should decline during the Late Miocene, especially between 8 and 3.5 Myr ago. The MAr record from the western Nepal foreland is consistent with this: muscovites from Upper Miocene–Pliocene strata in these basins yield only dates that are older than ~ 10 Myr ago (Fig. 2e). We interpret the first-order correlation between weathering records, erosion rates and cooling ages as suggestive of a genetic relationship between monsoon intensification and Himalayan exhumation in the Early Miocene. Such an interpretation is supported by the independent correlation of post-3.5 Myr ago monsoon strengthening with aggressive, Late Pliocene/Recent hinterland exhumation, as indicated by low-temperature thermochronometry³⁶ (see Supplementary Information, Methods).

ASIAN MONSOON STRENGTH AND HIMALAYAN EXHUMATION

The idea that mountain exhumation is linked to the intensity of monsoon precipitation provides a plausible answer to the question of why most of the deformational structures in the Himalaya are so much younger than initial India–Eurasia collision. In Early Miocene time, exhumation of the Himalayan hinterland was controlled by the displacement of two fault systems: the Main Central Thrust, currently exposed near the foot of the physiographic Higher Himalaya, and the South Tibetan fault (STF) system, which includes numerous low-angle normal faults that crop out near the range crest³⁷. Both fault systems dip shallowly northward, such that the Greater Himalayan sequence forms an inclined channel bound on the top and base by the two fault systems (Fig. 3). These fault systems accommodated southward extrusion and exhumation of the Greater Himalaya during the Early Miocene³⁸, a process often referred to as ‘channel flow’.

Noting that the Greater Himalayan sequence represents exhumed middle- to lower-crustal rocks, similar to those that might occur at depth beneath the Tibetan plateau, Nelson *et al.*³⁹ suggested that the Greater Himalayan channel had been extruded from beneath the plateau. This process could be driven by the excess gravitational potential energy of an over-thickened Tibetan crust if aggressive erosion occurred at the southern (Himalayan) margin of the plateau^{40,41}. If channel flow is driven by erosionally mediated gravitational collapse of the Tibetan plateau⁴⁰, then Himalayan

deformation is not only driven by India–Eurasia convergence, but also by the dynamics of Tibetan plateau evolution and its impact on the monsoon climate that is the principle control on erosion along the Himalayan front. It should be noted that alternative ‘critical wedge’ models for development of the Himalaya⁴² also invoke focused erosion to bring deeply buried rocks to the surface at the Himalayan front in the recent past and thus also predict a close relationship between monsoon rainfall and tectonic architecture.

Climate models have shown that the Tibetan plateau is likely to have strongly influenced the strengthening of the Asian monsoon climate^{43,44}. We suggest that the plateau had grown to sufficient size and elevation by Early Miocene time to permit both channel flow through deformation on the MCT and STF systems, and the strengthening of the monsoon to the extent that heavy summer rains began to fall on the southern edge of the plateau. Throughout the remainder of the Neogene, a high plateau and a persistent monsoon have maintained this essential architecture of the Himalaya, although temporal variations in monsoon intensity and/or India–Eurasia convergence rate might have induced mesoscale variations in the structural configuration. Late Miocene weakening of the summer monsoon would be responsible for the slower exhumation rates after ~10 Myr ago, possibly linked to global cooling after the Middle Miocene climatic optimum²³. An acceleration in exhumation and erosion after about 4 Myr ago^{29,35} correlates with strengthening of the monsoon since that time.

Further tests of the hypothesis that Himalayan hinterland uplift is genetically linked to monsoon strengthening require better resolution of the Cenozoic climate in the northern Indian subcontinent, as well as the rates of erosional flux to the ocean. Unfortunately, the foreland basins of the Himalaya have provided palaeoclimatic data mostly for the Middle Miocene/Recent interval^{45,46}. This limitation underscores the need for further palaeoclimatic studies focused on the more complete sedimentary records of the Indus and Bengal submarine fans to the east and west of the subcontinent.

METHODS

In this study, we constrained monsoon intensity via weathering proxies based on major-element chemical analyses. Analyses are based on X-ray fluorescence (XRF) measurements of major elements, the operational details of which are provided in Supplementary Information, Methods. Two methods were used, one is conventional bulk sediment analyses, which are usually carried out at low resolution, but which yield accurate elemental concentrations, and another that is a whole-core, non-destructive method in which the core is processed through an XRF scanner. These scanner data are in the form of counts, rather than weight percentage but are powerful in showing trends in relative concentration at high resolution, because thousands of analyses are possible, allowing details in the sediment chemistry to be revealed. Conventional XRF data were used to calculate CIA (ref. 17) for Late Miocene/Pliocene cuttings from well Indus Marine A-1 (Fig. 2b; Supplementary Information, Table S1). The CIA is a standard proxy for the intensity of chemical weathering in sediments, based on the concentrations of water-immobile Al relative to Na, K and Ca. These data can be compared with existing XRF data from Site 1148 (ref. 24) and Site 718 (ref. 27). Unfortunately, the whole-core XRF method is unable to measure Na so that this proxy could not be determined from that data set. Instead we plotted K/Al, as a measure of mobile versus immobile elements. We also plotted this ratio using the bulk sediment XRF data as a comparison (Fig. 2a–c).

In the case of the Site 1148 core, we derived a proxy (C_{RAT}) based on visible-light diffuse reflectance spectrophotometry data. C_{RAT} represents the ratio of chlorite/chlorite+haematite+goethite which can be determined based on identification of certain wavelengths characteristic of these minerals and which can be isolated using endmember mixing statistics (see Supplementary Information, Table S2). The C_{RAT} ratio is important because these are environmentally sensitive minerals. Chlorite is a product of physical erosion, whereas haematite and goethite are largely produced by chemical weathering⁴⁷.

Because the Site 1148 core had been scanned at high resolution of the diffuse reflectance spectrophotometry data, this allowed a high-resolution reconstruction of evolving clay mineralogy at this location to be made. All of the sediment is interpreted to be delivered to the continental margin from the neighbouring Pearl River drainage. Lower values of C_{RAT} imply more chemical weathering in the sediment source region than higher values. In tectonically stable southern China, chemical weathering intensity correlates with monsoon strength; with higher precipitation, the intensity of chemical weathering is greater and thus, in the sedimentary record, the C_{RAT} of eroded sediments should be lower. Details on the calculation of C_{RAT} are provided in Supplementary Information, Figs S3,S4.

Received 3 May 2008; accepted 10 October 2008; published 9 November 2008.

References

- Rowley, D. B. Age of initiation of collision between India and Asia: a review of stratigraphic data. *Earth Planet. Sci. Lett.* **145**, 1–13 (1996).
- Najman, Y. *et al.* Dating of the oldest continental sediments from the Himalayan foreland basin. *Nature* **410**, 194–197 (2001).
- DeCelles, P. G. *et al.* Detrital geochronology and geochemistry of Cretaceous–Early Miocene strata of Nepal: implications for timing and diachrony of initial Himalayan orogenesis. *Earth Planet. Sci. Lett.* **227**, 313–330 (2004).
- Hodges, K. V. *et al.* Thermobarometric and ⁴⁰Ar/³⁹Ar geochronologic constraints on Eohimalayan metamorphism in the Dinggye area, southern Tibet. *Contrib. Mineral. Petrol.* **117**, 151–163 (1994).
- Godin, L. *et al.* Crustal thickening leading to exhumation of the Himalayan metamorphic core of central Nepal: Insight from U–Pb geochronology and ⁴⁰Ar/³⁹Ar thermochronology. *Tectonics* **20**, 729–747 (2001).
- Ratschbacher, L. *et al.* Distributed deformation in southern and western Tibet during and after the India–Asia collision. *J. Geophys. Res.* **99**, 19917–19945 (1994).
- Yin, A. *et al.* Tertiary structural evolution of the Gangdese thrust system, southeastern Tibet. *J. Geophys. Res.* **99**, 18175–18201 (1994).
- Najman, Y. The detrital record of orogenesis: A review of approaches and techniques used in the Himalayan sedimentary basins. *Earth Sci. Rev.* **74**, 1–72 (2006).
- Clift, P. D. Controls on the erosion of Cenozoic Asia and the flux of clastic sediment to the ocean. *Earth Planet. Sci. Lett.* **241**, 571–580 (2006).
- Curry, J. R. Sediment volume and mass beneath the Bay of Bengal. *Earth Planet. Sci. Lett.* **125**, 371–383 (1994).
- Sun, X. & Wang, P. How old is the Asian monsoon system? Palaeobotanical records from China. *Palaeogeogr. Palaeoclimatol. Palaeoecol.* **222**, 181–222 (2005).
- Guo, Z. T. *et al.* Onset of Asian desertification by 22 Myr ago inferred from loess deposits in China. *Nature* **416**, 159–163 (2002).
- Garzzone, C. N., Ikari, M. J. & Basu, A. R. Source of Oligocene to Pliocene sedimentary rocks in the Linxia basin in northeastern Tibet from Nd isotopes: Implications for tectonic forcing of climate. *Geol. Soc. Am. Bull.* **117**, 1156–1166 (2005).
- Edmond, J. M. & Huh, Y. in *Tectonic Climate and Climate Change* (ed. Ruddiman, W. F.) 330–353 (Plenum, 1997).
- White, A. F. & Blum, A. E. Effects of climate on chemical weathering in watersheds. *Geochim. Cosmochim. Acta* **59**, 1729–1747 (1995).
- West, A. J., Galy, A. & Bickle, M. J. Tectonic and climatic controls on silicate weathering. *Earth Planet. Sci. Lett.* **235**, 211–228 (2005).
- Nesbitt, H. W. & Young, G. M. Early Proterozoic climates and plate motions inferred from major element chemistry of lutites. *Nature* **299**, 715–717 (1982).
- Singh, S. K., Sarin, M. M. & France-Lanord, C. Chemical erosion in the eastern Himalaya; major ion composition of the Brahmaputra and $\delta^{13}\text{C}$ of dissolved inorganic carbon. *Geochim. Cosmochim. Acta* **69**, 3573–3588 (2005).
- Galy, A. & France-Lanord, C. Higher erosion rates in the Himalaya: Geochemical constraints on riverine fluxes. *Geology* **29**, 23–26 (2001).
- Wang, P. *et al.* Site 1148. *Proc. Ocean Drill. Prog., Init. Rep.* **184**, 121 (2000).
- Li, X. *et al.* Geochemical and Nd isotopic variations in sediments of the South China Sea: a response to Cenozoic tectonism in SE Asia. *Earth Planet. Sci. Lett.* **211**, 207–220 (2003).
- Zheng, H. *et al.* Late Miocene and mid-Pliocene enhancement of the east Asian monsoon as viewed from the land and sea. *Glob. Planet. Change* **41**, 147–155 (2004).
- Zachos, J. *et al.* Trends, rhythms and aberrations in global climate 65 Ma to Present. *Science* **292**, 686–693 (2001).
- Wei, G. *et al.* Geochemical record of chemical weathering and monsoon climate change since the early Miocene in the South China Sea. *Paleoceanography* **21**, PA4214 (2006).
- France-Lanord, C., Derry, L. & Michard, A. in *Himalayan Tectonics* Vol. 74 (eds Treloar, P. J. & Searle, M. P.) 603–621 (Geological Society, 1993).
- Derry, L. A. & France-Lanord, C. Neogene Himalayan weathering history and river ⁸⁷Sr/⁸⁶Sr: impact on the marine Sr record. *Earth Planet. Sci. Lett.* **142**, 59–74 (1996).
- Crowley, S. F., Stow, D. A. V. & Croudace, I. W. in *Geological Evolution of Ocean Basins: Results from the Ocean Drilling Program* Vol. 131 (eds Cramp, A. *et al.*) 151–176 (Geol. Soc. Lond., spec. publ., Geological Society, 1998).
- Chakraborty, A., Nanjundiah, R. S. & Srinivasan, J. Role of Asian and African Orography in Indian Summer Monsoon. *Geophys. Res. Lett.* **29** doi:10.1029/2002GL015522 (2002).
- Metivier, F. *et al.* Mass accumulation rates in Asia during the Cenozoic. *Geophys. J. Int.* **137**, 280–318 (1999).
- Cochran, J. R. in *Proc. Ocean Drill. Prog., Sci. Rep.* Vol. 116 (eds Cochran, J. R. & Stow, D. A. V.) 397–414 (Ocean Drilling Program, College Station, 1990).
- Burbank, D. W., Derry, L. A. & France-Lanord, C. Reduced Himalayan sediment production 8 Myr ago despite an intensified monsoon. *Nature* **364**, 48–50 (1993).
- Hodges, K. in *The Crust* (ed. Rudnick, R.) 263–292 (Elsevier, 2003).
- Szulc, A. G. *et al.* Tectonic evolution of the Himalaya constrained by detrital ⁴⁰Ar/³⁹Ar, Sm/Nd and petrographic data from the Siwalik foreland basin succession, SW Nepal. *Basin Res.* **18**, 375–391 (2006).
- Reiners, P. W. & Brandon, M. T. Using thermochronology to understand orogenic erosion. *Annu. Rev. Earth Planet. Sci.* **34**, 419–466 (2006).
- Huntington, K. W., Blythe, A. E. & Hodges, K. V. Climate change and late Pliocene acceleration of erosion in the Himalaya. *Earth Planet. Sci. Lett.* **252**, 107–118 (2006).

36. Thiede, R. C. *et al.* Climatic control on rapid exhumation along the Southern Himalayan Front. *Earth Planet. Sci. Lett.* **222**, 791–806 (2004).
37. Hodges, K. V. Tectonics of the Himalaya and southern Tibet from two perspectives. *Geol. Soc. Am. Bull.* **112**, 324–350 (2000).
38. Burchfiel, B. C. *et al.* *Geol. Soc. Am. Spec. Pap.* 269, 41 (Geological Society of America, 1992).
39. Nelson, K. D. *et al.* Partially molten middle crust beneath southern Tibet; synthesis of Project INDEPTH results. *Science* **274**, 1684–1688 (1996).
40. Beaumont, C. *et al.* Himalayan tectonics explained by extrusion of a low-viscosity crustal channel coupled to focused surface denudation. *Nature* **414**, 738–742 (2001).
41. Hodges, K., Hurtado, J. & Whipple, K. Southward extrusion of Tibetan crust and its effect on Himalayan tectonics. *Tectonics* **20**, 799–809 (2001).
42. Robinson, D. M., DeCelles, P. G. & Copeland, P. Tectonic evolution of the Himalayan thrust belt in western Nepal; implications for channel flow models. *Geol. Soc. Am. Bull.* **118**, 865–885 (2006).
43. Kitoh, A. Effects of mountain uplift on east Asian summer climate investigated by a coupled atmosphere–ocean GCM. *J. Clim.* **17**, 783–802 (2004).
44. An, Z. *et al.* Evolution of Asian monsoons and phased uplift of the Himalaya–Tibetan Plateau since late Miocene times. *Nature* **411**, 62–66 (2001).
45. Behrensmeier, A. K. *et al.* The structure and rate of late Miocene expansion of C4 plants: Evidence from lateral variation in stable isotopes in paleosols of the Siwalik Group, northern Pakistan. *Geol. Soc. Am. Bull.* **119**, 1486–1505 (2007).
46. Ganjoo, R. K. & Shaker, S. Middle Miocene pedological record of monsoonal climate from NW Himalaya (Jammu & Kashmir State), India. *J. Asian Earth Sci.* **29**, 704–714 (2007).
47. Thiry, M. Palaeoclimatic interpretation of clay minerals in marine deposits: an outlook from the continental origin. *Earth Sci. Rev.* **49**, 201–221 (2000).
48. Gradstein, F. M., Ogg, J. G. & Smith, A. G. *A Geologic Time Scale* (Cambridge Univ. Press, 2004).
49. Shipboard Scientific Party, in *Proc. Ocean Drill. Prog., Init. Rep.* Vol. 184, (2000).
50. Gartner, S. Neogene calcareous nannofossil biostratigraphy, Leg 116 (Central Indian Ocean), in *Proc. Ocean Drill. Prog., Sci. Rep.* Vol. 116, 165–187 (1990).

Supplementary Information accompanies the paper at www.nature.com/naturegeoscience.

Acknowledgements

P.D.C. thanks the A. von Humboldt Foundation for the time to work on this study. K.V.H. thanks the US National Science Foundation for supporting this research through EAR0087508, EAR0642731 and EAR0708714 through its Continental Dynamics, Sedimentary Geology and Paleobiology, and Tectonics programs.

Author contributions

P.D.C. was responsible for deriving marine sedimentation rates and synthesizing the data. K.V.H. compiled thermochronology data and related the weathering to Himalayan tectonic history. D.H. generated the C_{RAT} weathering proxy and processed colour spectral data. R.H. produced the whole-sediment XRF data, and H.V.L. and G.C. were responsible for the whole-core XRF scanner data.

Author information

Reprints and permissions information is available online at <http://npg.nature.com/reprintsandpermissions>. Correspondence and requests for materials should be addressed to P.D.C.